Journal of King Saud University – Science 32 (2020) 1503–1509

Contents lists available at ScienceDirect

Journal of King Saud University – Science

journal homepage: www.sciencedirect.com

Original article

Integrated approach: Al_2O_3-CaO nanocatalytic biodiesel production and antibacterial potential silver nanoparticle synthesis from *Pedalium murex* extract

G. Sivaprakash [a,b], K. Mohanrasu [a,c], B. Ravindran [d,*], Woo Jin Chung [d], Dunia A. Al Farraj [e], Mohamed Soliman Elshikh [e], Manal M. Al Khulaifi [e], Roua M. Alkufeidy [e], A. Arun [c,*]

[a] Department of Energy Science, Alagappa University, Karaikudi 630003, Tamil Nadu, India
[b] Vidhyaa Giri College of Arts and Science, Puduvayal 630108, Tamil Nadu, India
[c] Bioenergy and Bioremediation Laboratory, Department of Microbiology, Alagappa University, Karaikudi 630003, Tamil Nadu, India
[d] Environmental Energy and Engineering, Kyonggi University, Youngtong-Gu, Suwon 16227, Republic of Korea
[e] Botany and Microbiology Department, College of Sciences, King Saud University, P.O. Box 22452, Riyadh 11495, Saudi Arabia

ARTICLE INFO

Article history:
Received 29 September 2019
Revised 3 November 2019
Accepted 1 December 2019
Available online 16 December 2019

Keywords:
Pedalium murex
Nanocatalyst
Biodiesel
Lipid extraction
Antibacterial activity

ABSTRACT

Pedalium murex, a less-utilized traditional plant, has high lipid content, which ranges from 21 mg/gfw (milligram per gram fresh weight) in leaf, 32 mg/gfw in stem and 19 mg/gfw in callus. Lipids from different parts of the plant were extracted and employed for biodiesel production. Al_2O_3-CaO nanocatalyst was synthesized by the classical Sol-gel method, characterized by XRD, HR-SEM, and was applied for biodiesel production. In transesterification, the influence of methanol-lipid was evaluated by varying the ratio from 1:6 to 1:16, and the FAME converted yield was calculated to be 60% using Gas chromatography. The biomass was subjected to lipid extraction and was then used for the synthesis of AgNPs, analyzed through the UV–Visible absorption spectrum, XRD, HR-SEM, and SAED. AgNPs of Pedalium murex plant extract were examined for their antimicrobial activity against various bacterial pathogens such as *Staphylococcus aureus*, *Klebsiella pneumonia*, *Bacillus subtilis* and *Escherichia coli.* AgNPs showed the best antibacterial activity against *E. coli* at 5.0 mM concentration. This study is promising in the identification of a cheap source for biodiesel production with the added advantage of antimicrobial drug formulation from the medicinal plant Pedalium murex.

1. Introduction

Biodiesel has the great alternation instead of fossil fuel and great attention because of environmental compatibility and biodegradability (Aarthy et al., 2014; Chen et al., 2012; Reyero et al., 2014). *P. murex* is a member of Pedaliaceae commonly known as 'Gokshru' and is distributed throughout the world including, India, Srilanka, Paksistan and Africa (Patel et al., 2011). The plant materials were utilized by local people as an analgesic and antipyretic (Patel et al., 2011). Because of its important biological activities, medicinal applications and high lipid content in various parts of *P. murex*, we had chosen it as a suitable candidate for biomass utilization (SHARMA, n.d.). Evaluation of dietary effects of *P. murex* ethanolic extract was reported to be 9.5 kcal/g (Jobling, 1983; Ojha et al., 2014). Bligh and dyer method was applied with simple modifications such as the reduced quantity of solvent and obtained the maximum amount of lipids from different parts (leaf, stem, and callus) of *P. murex* (Ewald et al., 1998). The heterogeneous catalyst alumina supported calcium oxide was used in this study and was classically synthesized by a sol–gel method as described by Umdu et al. (2009). Among the solid base catalysts, CaO is economical with several advantages such as long catalytic lifetime, mild reaction conditions, high basicity, high activity and uses as a potent catalyst for effective synthesis of biodiesel (Wu et al., 2012). Adding Al_2O_3 as a supportive material will increase catalytic activity by many folds, especially suitable stability and dispersion properties with surface-enhanced

* Corresponding authors.
E-mail addresses: kalamravi@gmail.com (B. Ravindran), arunalacha@gmail.com (A. Arun).
Peer review under responsibility of King Saud University.

Production and hosting by Elsevier

https://doi.org/10.1016/j.jksus.2019.12.004
1018-3647/

reactant interactions (Galadima and Muraza, 2014). Whereas the Al_2O_3-CaO system yields the most promising activity because of higher basicity and site concentration (Umdu et al., 2009). The solid biomass (after lipid extraction) was utilized to synthesize silver nanoparticles (AgNPs). AgNPs possess antibacterial activity against types of pathogens because of Ag ions (Arokiyaraj et al., 2015; Moosavi et al., 2015; Valsalam et al., 2019a, 2019b; Gurusamy et al., 2019). In this study, the antimicrobial potential of synthesized AgNPs were screened against highly pathogenic bacteria such as, *Staphylococcus aureus, Escherichia coli, Bacillus subtilis* and *Klebsilla pneumonia*. This study detailed an optimized extraction of lipid content from different parts (leaf, stem and callus) of the commonly denoted traditional plant (*P. murex*) for the production of biodiesel catalyzed by Al_2O_3-CaO. The remaining biomass (after lipid extraction) was utilized for the synthesis of AgNPs with antibacterial potentiality.

2. Materials and methods

2.1. Preparation of catalyst and analytical technique

In this study catalyst was prepared as suggested by Yoldas (1975) and was used to synthesize CaO doped Al_2O_3 using Aluminum isopropoxide and Calcium nitrate as a precursor with 1:1 ratio. 10.2 g of Aluminum isopropoxide was added into 50 ml of 0.5 M HNO3, where placed in a reflux condenser with a silicon oil magnetic stirrer heating reactor at 85 °C for 1 h. To this, 8.2 g of Calcium nitrate was carefully added and continuously stirred till the formation of the gelly mixture. After 2 h of stirring, excess water was removed, and the gel was dried for 18 h at 120 °C and calcined for 6 h at 500 °C. The crystalline nature of synthesized catalysts were analyzed through X-ray diffraction and average crystalline size were calculated by debye scherrer equation. The foremost identifications and surface morphology characters of synthesized nanocatalyst was investigated by using High-resolution Scanning electron microscope (HR-SEM) incorporated with Energy-dispersive X-ray spectroscopy (EDAX).

2.2. Lipid extraction

P. murex plant was collected near the science campus of Alagappa University, Karaikudi Tamil Nadu, India (latitude: 10.094004, longitude: 78.785493). *P. murex* contains high lipid content ranging from 21 mg/gfw (milligram per gram fresh weight of tissues) in leaf, 32 mg/gfw in stem and 19 mg/gfw in callus (SHARMA, n.d.) were individually extracted as described by Kumari et al. (2011) with simple modification. All the analysis was made with 4 g of ground plant tissues. Using this method, lipids were successfully extracted from all parts of the *P. murex* plant and were transesterified by using Al2O3-CaO nanocatalyst. The biomass was washed with double distilled water after lipid extraction distilled water, further air dried and used for AgNPs synthesis for potential antibacterial application.

2.3. Transesterification of P. murex and FAME analysis

Transesterification process was mainly affected by reaction temperature, reaction time, methanol to oil molar ratio and catalyst concentration (Banković-Ilić et al., 2017; Baskar et al., 2017; Baskar and Soumiya, 2016; Sivaprakash et al., 2019; Zabeti et al., 2010). Optimization of different parameters were carried for FAME production like methanol-oil ratio from 1:6, 1:8, 1:10, 1:12, 1:14 & 1:16, different catalyst concentration from 5, 10, 15, 20, 25 & 30 wt % with reaction time frame of 2, 3, 4, 5, 6 & 7 h and different temperatures ranged between 40 °C and 90 °C with 10 °C interval. Methanol and lipid content were mixed vigorously in the reflux container under magnetic stirrer; Al_2O_3-CaO composite was gradually added to the above mixer. 2 ml of formaldehyde was added to 2 ml of supernatant and was characterized by gas chromatography (Shimadzu 2010, Japan). This instrument was equipped with a capillary column (105 m, 0.32 mm ID, 0.20 μm film thickness) and detected using a Flame ionization detector (FID). Injector temperature was maintained as 225 °C, whereas detector temperature was adjusted as 250 °C, respectively. 1 μl of the sample was carefully injected onto a FAMEs-RTX-2330 column (105.0 m length) using split mode (35:1) and the flow rate was 184.9 ml/min. GC solution software was used for a combination of peak areas and FAME was identified with internal standards.

2.4. Synthesis of AgNPs from remaining P. murex biomass

1 g of dried biomass (leaf, stems & callus) was kept in 30 ml of distilled water at 80 °C for 20 min. $AgNO_3$ was prepared at 1 mM concentration and was kept on magnetic stirrer for about 2 h at 80 °C for continuous stirring. Then, 10 ml of different extracted leaf biomass was added slowly with continuous stirring. The same procedure was followed to extract from stem and callus. AgNPs formation was confirmed by the appearance of brown color. *P. murex* contains various phytochemicals, including flavonoids, phenolics, terpenoids, glycosides and saponins and these phytochemicals involved in AgNPs synthesis (Sharma et al., 2012). Such functional groups provide a good reduction of silver ions to AgNps (Vijayan et al., 2014). The maximum absorption spectra of the synthesized AgNPs were characterized using UV–Visible spectroscopy (Shimadzu, Japan) and X-ray diffraction analysis (X'Pert PRO analytical X-ray diffractometer). The size of the synthesized NPs and morphology was analyzed by HR-SEM images. AgNPs sample was dropped over carbon-coated copper grid with 200 mesh size and allowed to dry before observation. The functional components of AgNPs were detected by Fourier Transform infrared spectroscopy (FT-IR) between 400 and 4000 nm (Nicolet 380 FTIR spectrometer).

2.5. AgNPs and its antibacterial property

The synthesized AgNPs were tested for its antibacterial activity at three different concentrations (5 μg/ml, 10 μg/ml, and 15 μg/ml) against bacterial cultures (*K. pneumonia*, *B. subtilis*, *E. coli* and *S. aureus*) procured from MTCC. In this study, Mueller Hinton Agar was used for the determination of antibacterial activity as described by Ruparelia et al. (2008). All plates were incubated at 37 °C for 24 h and inhibitory activities were observed. The results were compared with standard antibiotics.

3. Results and discussion

To the best of our knowledge, there is no report on the biodiesel production from *P. murex* by using heterogeneous catalysts. In this study, Al_2O_3 and CaO_4 were synthesized individually, compared with Al_2O_3-CaO and XRD pattern is described Fig. 1. Fig. 1(a) shows Al_2O_3-CaO mixed metal oxide. Al_2O_3 and CaO_4 were perfectly matched with ICDD card no: 000020921, 000210155, respectively (Fig. 1b and c).

The peak broadening, average particle size of Al_2O_3, CaO_4 and Al_2O_3-CaO were calculated by Debey–Scherrer formula, Al_2O_3 having particle size of 30 nm is formed in hexagonal crystal system, CaO_4 pure and Al_2O_3-CaO were amorphous in nature, thus particle size were 20–30 nm. Small peaks integration (>5 nm) (Umdu et al., 2009) in XRD is improbable and thickness of crystalline substance must be large to calculate the average size of CaO and Al_2O_3-CaO.

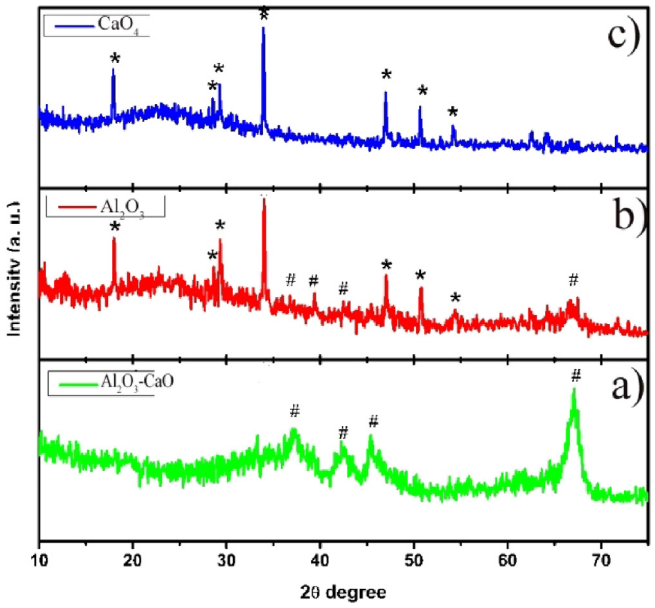

Fig. 1. a) XRD Pattern of Al_2O_3-CaOnanocomposite b) CaO_4 c) Al_2O_3 nanocomposite.

In our study we observed spherical rod-shaped mixed oxide catalyst in HR-SEM (Fig. 2), but it could not be observed in XRD.

Heterogeneous basic catalysts will selectively yield higher products than other catalysts in free fatty acids and the yield of biodiesel will decrease when froth formation occurs (Lam et al., 2010). Some recent research were achieved as high as 94%, FAME yield from the, composites of Al_2O_3 revealed the presence of metal oxides like $LiNO_3/Al_2O_3$, $NaNO_3/Al_2O_3$, $CrOx/Al_2O_3$, $MoOx/Al_2O_3$, WOx/Al_2O_3 and $MoOx/P\text{-}Al_2O_3$(Satyarthi, 2011)furthermore those materials demands calcinations at <450 °C (Kumar et al., 2012). Water component reacts with alkyl esters forming carboxylic acids that react with alkaline metals, resulting in sodium or potassium salts (soap formation) which in turn reduces alkyl ester yield and makes recovery of glycerol complicated (Freedman et al., 1986). In a study, Noiroj et al. (2009) used palm oil under transesterification process by using 25 wt% of KOH loaded Al_2O_3 catalyst yields 91% conversion at 70 °C from methanol to oil molar ratio of 1:15. Mixed catalyst of CaO and ZnO were studied with very large surface area and small particle size to increase the FAME yield up to 94% from 10% wt of catalysts at 60 °C with an hour of incubation (Ngamcharussrivichai et al., 2008). Zabeti et al. (2009) used Al_2O_3-CaO composite catalyst in transesterification process in palm oil and showed significant positive effects on the presence of calcium oxide. In another study, similarly synthesized CaO catalysts were utilized for transesterification from Jatropha oil and yield 95% (Hawash and Diwani, 2011). CaO nanocatalysts consist of high surface area associated with nanocrystalline nature, which enhances the reaction kinetics (Banković-Ilić et al., 2017).

Mixed catalyst of CaO and ZnO were studied with small particle size and higher surface area to increase the FAME yield up to 94% from 10% wt of catalysts at 60 °C with an hour of incubation (Ngamcharussrivichai et al., 2008).

The size and shape of metal oxide CaO_4, Al_2O_3 and composite Al_2O_3-CaO was determined. The particle size of the Al_2O_3-CaO was 25–30 nm (99%), specific surface area (SSA) was 70–82.74 m_2/g and active site concentration was 190 μmol/g conducted by TPD-CO_2 test method.

In the optimization of transesterification reaction, methanol to oil molar ratio leads a major role in FAME conversion. Transesterification requires 3 mol concentration of methanol to get yield the same amount of fatty acids and one mol of glycerol in stoichiometry ratio (Baskar and Soumiya, 2016). Catalyst concentration induces the reaction rate; oil molar ratio deals the impacts in reaction reversible, reaction temperature control the evaporation of methanol and nanocatalysts methyl ester conversion is directly proportional to reaction time (Maceiras et al., 2011; Baskar et al., 2017). Reaction was carried using various molar ratios (1:6, 1:8, 1:10, 1:12, 1:14 & 1:16) under the conditions of varying catalyst concentration (5, 10, 15, 20, 25 & 30 wt%), incubation temperatures (40 °C – 90 °C) and reaction time (2, 3, 4, 5, 6 & 7 h). The Optimization of various parameters (Effect of conversion in oil molar ratio, Catalysts wt %, Temperature °C, Time h) on FAME conversion from *P. murex* lipid was mentioned in Table 1.

CaO has been used recognized as catalyst for transesterification process (Banković-Ilić et al., 2017). Catalyst concentration enhances the conversion yield in the transesterification process. While increasing the wt % of catalysts results in a significantly increased quantity of biodiesel yield. Highest biodiesel conversion was recorded at 25 wt% of catalyst, a higher amount of catalyst made a slurry-like substance that required increased stirring with more power consumption (Ayetor et al., 2015). Moreover, the reusability of catalysts was also checked for 25 wt% of catalysts after transesterification and delivered good performance for further two tests.

After completion of the reaction, supernatant (methyl esters) was collected and a similar amount of *ortho*-phosphoric acid was added and thereafter characterized by Gas chromatography. The stability of the catalyst must be good in the reusability concept (Baskar et al., 2017).

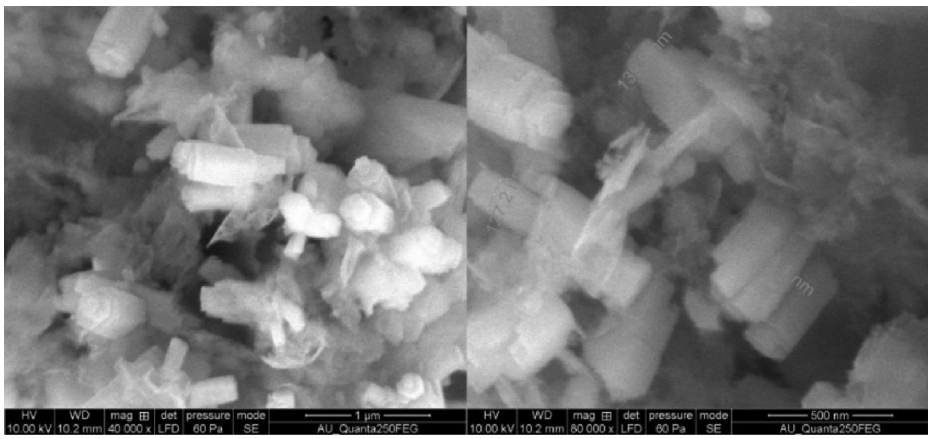

Fig. 2. HR-SEM results of Al_2O_3-CaO nanocomposite.

Table1
Optimization of various parameters (oil molar ratio between 1:6–1:16, catalysts between 5 and 25 wt%, temperature between 40 and 90 °C, time between 2 and 7 h) on FAME yieldand triglyceride conversionfrom *P. murex* lipid.

Oil molar ratio																																							
Catalysts Wt %		1:6					1:8					1:10					1:12					1:14					1:16											
		5	10	15	20	25	5	10	15	20	25	30	5	10	15	20	25	30	5	10	15	20	25	30	5	10	15	20	25	30	5	10	15	20	25	30	5	10	15	20	25	30
Temp °C/6h	40	13	16	17	17	19	20	22	23	24	24	28	28	31	32	34	35	36	35	38	37	38	39	45	46	45	47	48	50	52	55	52	54	53	53	55	55	55	55	56	56	56
	50	14	17	18	18	20	20	23	23	23	25	28	29	32	33	35	36	37	36	38	38	39	40	46	47	46	47	49	52	54	56	53	53	54	55	56	56	57	54	55	57	57
	60	15	17	19	19	21	21	23	23	24	25	29	30	32	32	35	37	37	37	39	39	39	41	47	48	47	48	50	51	56	57	54	55	55	56	57	57	56	54	57	57	57
	70	15	18	19	20	22	22	23	25	26	29	30	31	33	33	36	37	37	38	38	40	40	42	47	48	47	48	51	53	58	58	55	56	56	57	58	58	57	56	58	58	58
	80	16	19	20	21	22	24	24	26	26	30	31	33	34	34	36	37	38	40	40	41	42	44	48	49	48	49	51	54	60	60	55	56	57	57	57	58	58	58	59	59	59
	90	16	19	19	20	21	21	24	24	26	27	30	30	34	34	35	36	37	38	40	41	42	45	48	48	46	47	48	50	53	56	53	54	53	54	55	55	55	54	55	57	56
Time (h)/80 °C	2	12	16	17	17	19	19	22	22	23	24	28	28	31	32	34	35	36	35	38	37	38	39	45	46	45	47	49	50	55	57	52	55	54	55	57	57	55	54	55	57	56
	3	13	17	18	18	20	20	22	23	23	25	28	29	33	33	35	36	37	35	38	38	39	40	46	47	46	47	48	50	55	57	52	55	55	55	57	57	55	55	56	57	57
	4	15	15	18	19	21	21	23	23	23	25	29	28	32	33	34	37	36	37	37	39	38	42	46	48	48	48	50	51	57	57	55	55	55	56	57	57	57	55	56	57	57
	5	14	18	19	21	22	23	23	25	25	28	30	33	33	34	36	37	37	39	41	42	43	47	48	49	49	48	51	53	59	58	55	55	56	56	57	58	57	56	57	58	58
	6	16	19	18	21	22	24	24	26	27	30	31	33	34	34	35	37	38	41	42	41	43	48	49	49	49	49	53	54	60	60	56	56	57	57	58	58	57	57	58	58	59
	7	16	19	19	20	21	21	24	24	26	27	30	30	34	34	34	37	38	40	41	41	45	48	49	48	48	49	52	56	60	60	56	57	57	56	58	59	58	58	59	59	59

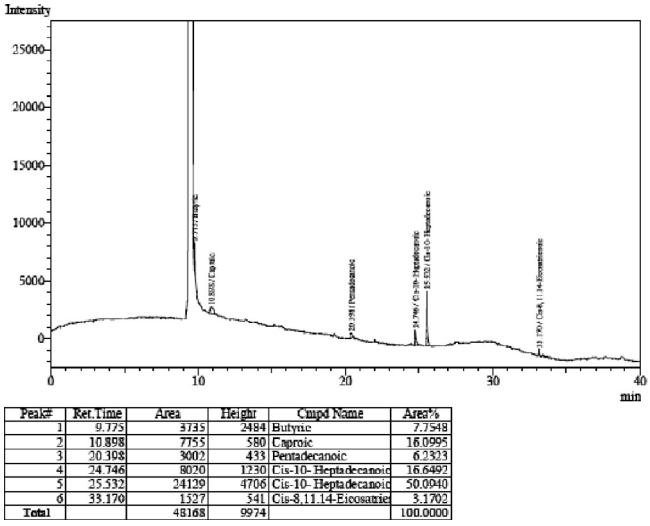

Peak#	Ret.Time	Area	Height	Cmpd Name	Area%
1	9.775	3735	2484	Butyric	7.7548
2	10.898	7755	580	Caproic	16.0995
3	20.308	3002	433	Pentadecanoic	6.2323
4	24.746	8020	1230	Cis-10- Heptadecanoic	16.6497
5	25.532	24129	4706	Cis-10- Heptadecanoic	50.0940
6	33.170	1527	541	Cis-8,11,14-Eicosatrien	3.1702
Total		48168	9974		100.0000

Fig. 3. Gas chromatography analysis of fatty acid methyl ester.

From the analyzed FAME by GC, (Fig. 3) it was determined that saturated fatty acid content is higher whilst undesirable poly unsaturated fatty acids are less.

Major components identified are Cis-10-Heptadecanoic acid methyl ester (C17:1), Eicosadienoic acid methyl ester (C20:2) 8.43%, moreover apart from these major FAME components we observed Butyric acid (C4:1) 5.53%, Caproic acid (C6:1) 11.53%, Pentadecanoic acid (C15:1) 18.17% Palmitic acid (C16:0) 3.941%, Octadecenoic (C18:1) 54.5831%, Hexadecenoic (C16:1) 6.941%, Stearidonic acid (C18:4x3) 3.39%, Linoleic acid (C18:2) 4.45% and the total Saturated fatty acid 65.8%, Polyunsaturated fatty acid 6.2%. The properties of biodiesel, such as Saponification value 150 ml of H_3PO_4/g, Iodine value 96, Acid value 10 ml of H_3PO_4/g, water content 2.7%/ml, sulphated ash 0.009%/ml and density. 89%/ml was also determined through ASTM standards (Table 2). In the conversion of FAME beyond the double bond was the impact of γ-alumina. A notable increment in the results observed behind the double bond in the conversion of methyl soyate.

After lipid extraction, the obtained biomass was utilized to synthesize AgNPs. The silver nitrate color was completely changed from pale-yellow to brownish while adding the *P. murex* extract at an incubation temperature of 80° C. The spectral data results from existing characteristic SPR due to the reduction of silver ions. UV–Visible spectrum analysis revealed a peak corresponding to 435 nm (Fig. 4). For the control with plain extract shows the peaks at 280–300 nm. Results were reliable with high intensity peak absorbance with small peak width at prominent temperatures.

The phytochemicals of *P. murex* effectively reduced silver nitrate into AgNPs. X-Ray diffraction was performed for synthesized AgNPs to confirm the crystalline nature. XRD pattern shows the distinct peaks at 38.2°, 44.4°, 64.6°, 77.5° and 81.7 for the AgNPs synthesized from *P. murex* extract after lipid extraction.

Table 2
Physical and chemical properties of produced biodiesel with ASTM standards.

Parameters	Extracted plant oil	Units
Average molecular weight	840	g/mol
Saponification value	150	ml of H_3PO_4/g
Iodine value	96	–
Acid value	10	ml of H_3PO_4/g
Water content	2.7	%/ml
Sulphated ash	0.009	%/ml
Density	0.89	%/ml

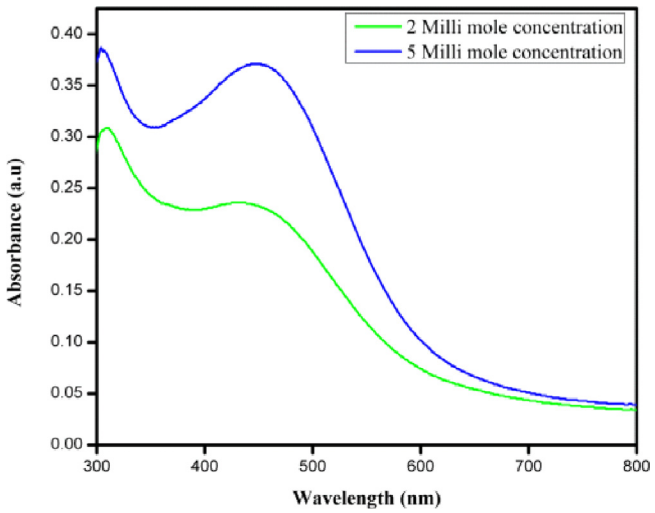

Fig. 4. UV–Vis spectra of silver nanoparticles synthesized from left over biomass of *P. murex*.

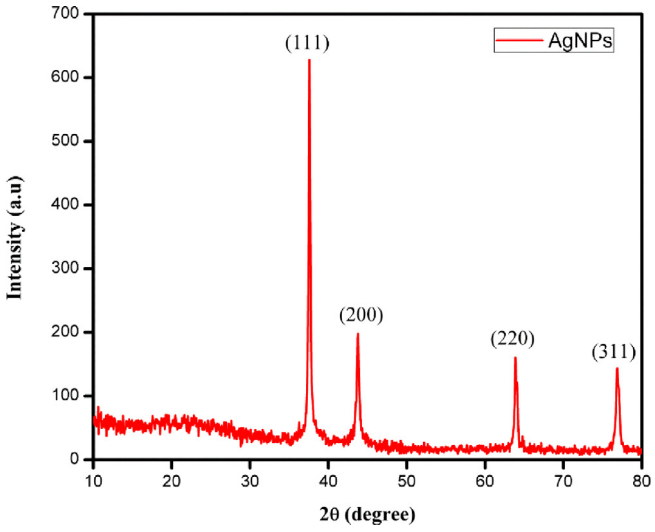

Fig. 5. XRD Pattern of silver nanoparticles synthesized from left over biomass of *P. murex* extract.

The observed lattice parameters were 111, 200, 220, 311, and 222 confirms the cubic silver (Fig. 5).

The calculated lattice constant was perfectly matched with ICDD card number: 01-087-0718. It suggests the formation of AgNPs from the *P. murex* extract and emphatically proved the crystalline phase presence in HR-SEM (Fig. 6). EDAX (energy dispersive X-ray analysis) (Fig. 7) of the AgNPs sample showed the existence of silver (Ag) element in the sample, moreover, other peaks shown are from the substrate, because of the diffusion of high-energy X-rays inside the sample.

From the results of Fourier Transform infrared spectroscopy, the broad spectrum clearly shows the peak shift at 3428 cm^{-1} shows O–H stretching frequency mainly due to free hydroxyl groups in the sample. Also, a broad spectrum was observed at 1635 cm^{-1} due to carboxylic acid group. At 1049 cm^{-1}, a band was observed which confirmed the presence of alcohol groups and C–OH vibrations (Fig. 8). AgNPs showed potent activity against *K. pneumonia*, *B. subtilis*, *E. coli* and *S. aureus* (Fig. 9). The inhibitory effect of AgNPs on Gram-positive and Gram-negative bacteria was described in Table 3.

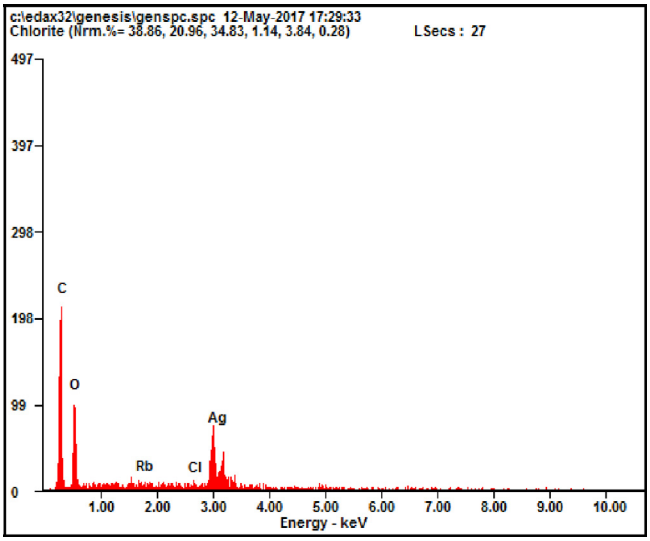

Fig. 7. EDAX results of synthesized silver nanoparticles.

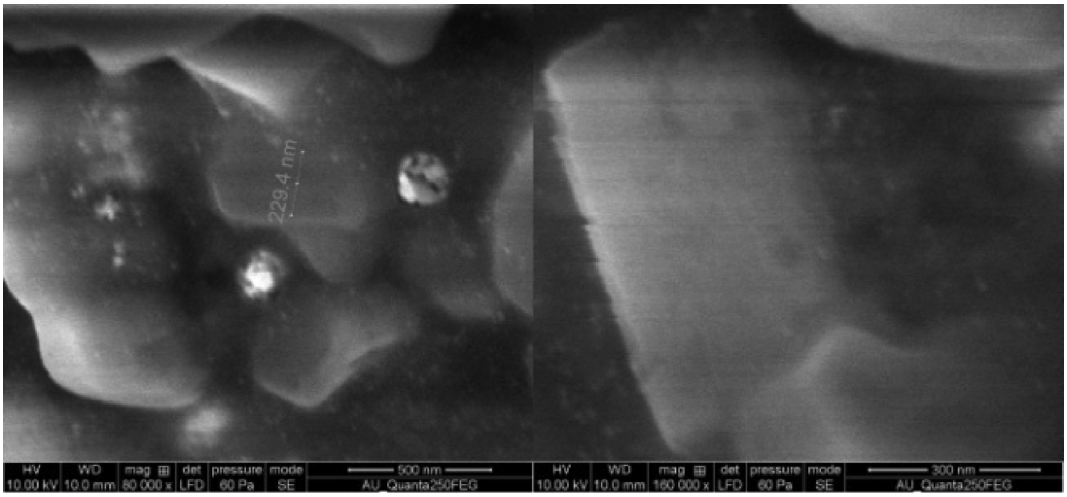

Fig. 6. HR-SEM images of silver nanoparticles synthesized from left over biomass of *P. murex*.

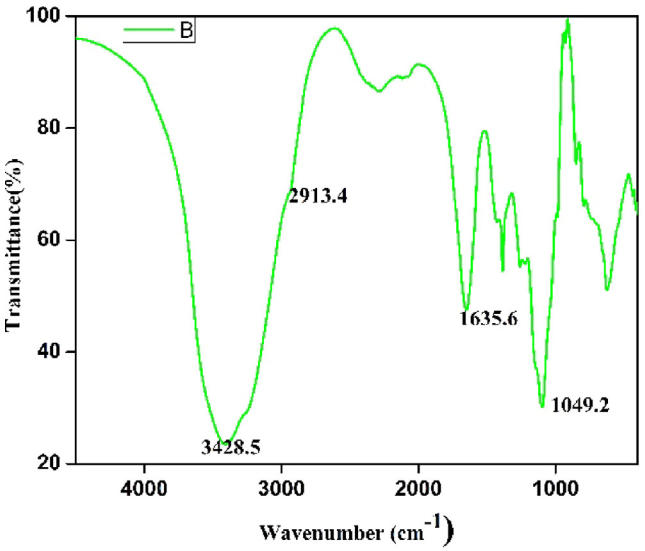

Fig. 8. FT-IR results of AgNps synthesized from the leftover *P. murex* extract.

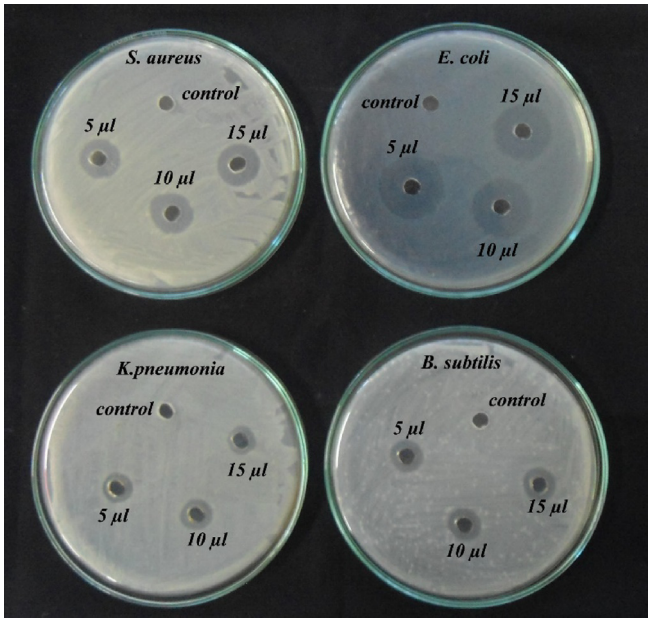

Fig. 9. Antibacterial efficiency of synthesized silver nanoparticles.

Antibacterial activity was found to be high against Gram-negative *E. coli* (11 mm); this maximum inhibition is due to the penetration of NPs through cell membrane in Gram negative bacterial cell walls and makes penetration much easier when compared with gram positive bacteria (Shrivastava et al., 2010; Al-Dhabi and Ghilan, 2019; Al-Dhabi et al., 2018) But the mechanism of inhibition behind the antibacterial ability of AgNPs is not yet fully elucidated (Shao et al., 2015; Rajkumari et al., 2019; Arasu et al., 2019) AgNPs release Ag+ ions and these ions bind enzymes and proteins of the cell surface of bacteria and suppress cell division and replication cause bacterial cell death (Franchini et al., 2014). AgNPs exhibits less impact on Gram-positive bacteria than Gram-negative bacteria resulting in the destruction of *E. coli* cell membrane or wall integrity (Tang et al., 2013).

4. Conclusions

Summary illustrates the environmental prosperity of biodiesel production using lipid extracted from *P. murex*. The reaction was performed by applying Al_2O_3-CaO nanocatalysts synthesized by sol–gel method. It was obtained maximum lipid extraction of 21 mg/gfw from leaf, 32 mg/gfw from stem and 19 mg/gfw from callus and was utilized for biodiesel production. We also found that Al_2O_3-CaO nanocomposite is a promising candidate for highly efficient catalytic activity rather than pure Al_2O_3, CaO_4. A 60% conversion was attained at 1:14 oil molar ratio with 25 wt% catalysts loading at incubation of 80 °C and 6 h of reaction time. The remaining biomass (after lipid extraction) was utilized for the synthesis of cubic AgNPs as a potential biogenic antibacterial drug. The synthesized AgNPs showed maximum zone of inhibition against *E. coli*. Thus we conclude *P. murex*, a common medicinal plant in India, has potential for large scale production of biodiesel in the presence of Al_2O_3-CaO catalysts and the leftover biomass proved to be a suitable substrate for synthesis of AgNPs which acts as an efficient antibacterial agent.

Declaration of Competing Interest

The authors declare that they have no known competing financial interests or personal relationships that could have appeared to influence the work reported in this paper.

Acknowledgements

Authors are gratefully acknowledging Department of Science and Technology-Promotion of University Research and Scientific Excellence (DST-PURSE) (DST letter No.SR/PURSE phase 2/38(G), dt.21.02.2017), India. Alagappa University Research Fund, Alagappa University (AURF) Interdepartmental Project Scheme, 2017, RUSA – Phase 2.0 grant sanctioned vide Letter No. F.24-51/2014-U, Policy (TNMulti-Gen), Dept. of Edn. Govt. of India, Dt.09.10.2018 and University Science Instrumentation Centre (USIC), Alagappa University, Karaikudi, Tamil Nadu, India. The authors would like to thank the Deanship of Scientific Research at King Saud University for funding this work through research

Table 3
Antibacterial activities of AgNPs synthesized from leftover *P. murex* extract.

S.No	Pathogens	Zone of inhibition (mm) of 5 mol concentration of synthesized AgNPs			Ag+ & culture	Zone of inhibition of commercial antibiotics							
		5 µl	10 µl	15 µl	Positive control	Tetracycline	Ampicillin	Clindamycin	Gentamicin	Teicoplanin	Vancomycin	Erythromycin	Penicillin
1.	*S. aureus*	5	6	8	7	17	20	–	25	10	–	25	–
2.	*E. coli*	9	10	11	9	–	15	–	20	20	–	10	–
3.	*B. subtilis*	6	7	7	7	10	17	–	25	10	–	25	–
4.	*K.pneumoniae*	5	6	7	6	15	10	–	15	–	–	20	–

group no. RG1439-044.The authors would like to thank the Deanship of Scientific Research at King Saud University for funding this work through research group no. RG1439-044.

References

Aarthy, M., Saravanan, P., Gowthaman, M.K., Rose, C., Kamini, N.R., 2014. Enzymatic transesterification for production of biodiesel using yeast lipases: An overview. Chem. Eng. Res. Des. 92, 1591–1601. https://doi.org/10.1016/j.cherd.2014.04.008.

Al-Dhabi, N.A., Ghilan, A.K.M., Arasu, M.V., Duraipandiyan, V., Ponmurugan, K., 2018. Environmental friendly synthesis of silver nanomaterials from the promising Streptomyces parvus strain Al-Dhabi-91 recovered from the Saudi Arabian marine regions for antimicrobial and antioxidant properties. J. Photochem. Photobiol. B: Biol. 189, 176–184.

Al-Dhabi, N.A., Ghilan, A.K.M., Arasu, M.V., Duraipandiyan, V., 2019. Green biosynthesis of silver nanoparticles produced from marine Streptomyces sp. Al-Dhabi-89 and their potential applications against wound infection and drug resistant clinical pathogens. J. Photochem. Photobiol., B: Biol. 111529

Arasu, M.V., Arokiyaraj, S., Viayaraghavan, P., Kumar, T.S.J., Duraipandiyan, V., Al-Dhabi, N.A., Kaviyarasu, K., 2019. One step green synthesis of larvicidal, and azo dye degrading antibacterial nanoparticles by response surface methodology. J. Photochem. Photobiol., B 190, 154–162.

Arokiyaraj, S., Saravanan, M., Badathala, V., 2015. Green synthesis of Silver nanoparticles using aqueous extract of Taraxacum officinale and its antimicrobial activity. South Ind. J. Biol. Sci. 2, 115–118.

Ayetor, G.K., Sunnu, A., Parbey, J., 2015. Effect of biodiesel production parameters on viscosity and yield of methyl esters: Jatropha curcas, Elaeis guineensis and Cocos nucifera. Alexandria Eng. J. 54, 1285–1290.

Banković-Ilić, I.B., Miladinović, M.R., Stamenković, O.S., Veljković, V.B., 2017. Application of nano CaO–based catalysts in biodiesel synthesis. Renew. Sustain. Energy Rev. 72, 746–760.

Baskar, G., Gurugulladevi, A., Nishanthini, T., Aiswarya, R., Tamilarasan, K., 2017. Optimization and kinetics of biodiesel production from Mahua oil using manganese doped zinc oxide nanocatalyst. Renew. Energy 103, 641–646.

Baskar, G., Soumiya, S., 2016. Production of biodiesel from castor oil using iron (II) doped zinc oxide nanocatalyst. Renew. Energy 98, 101–107.

Chen, Y.-H., Huang, B.-Y., Chiang, T.-H., Tang, T.-C., 2012. Fuel properties of microalgae (Chlorella protothecoides) oil biodiesel and its blends with petroleum diesel. Fuel 94, 270–273.

Ewald, G., Bremle, G., Karlsson, A., 1998. Differences between Bligh and Dyer and Soxhlet extractions of PCBs and lipids from fat and lean fish muscle: Implications for data evaluation. Mar. Pollut. Bull. 36, 222–230.

Franchini, C.A., Aranzaez, W., Duarte de Farias, A.M., Pecchi, G., Fraga, M.A., 2014. Ce-substituted LaNiO3 mixed oxides as catalyst precursors for glycerol steam reforming. Appl. Catal. B Environ. 147, 193–202. https://doi.org/10.1016/j.apcatb.2013.08.036.

Freedman, B., Butterfield, R.O., Pryde, E.H., 1986. Transesterification kinetics of soybean oil 1. J. Am. Oil Chem. Soc. 63, 1375–1380.

Galadima, A., Muraza, O., 2014. Biodiesel production from algae by using heterogeneous catalysts: A critical review. Energy. 0–11.

Gurusamy, S., Kulanthaisamy, M.R., Hari, D.G., Veleeswaran, A., Thulasinathan, B., Muthuramalingam, J.B., Balasubramani, R., Chang, S.W., Arasu, M.V., Al-Dhabi, N.A., Selvaraj, A., Alagarsamy, A., 2019. Environmental friendly synthesis of TiO2-ZnO nanocomposite catalyst and silver nanomaterials for the enhanced production of biodiesel from Ulva lactuca seaweed and potential antimicrobial properties against the microbial pathogens. J. Photochem. Photobiol., B 193, 118–130.

Jobling, M., 1983. A short review and critique of methodology used in fish growth and nutrition studies. J. Fish Biol. 23, 685–703.

Kumar, A., Osembo, S.O., Namango, S.S., Kiriamiti, K.H., 2012. Heterogeneous Basic Catalysts for Transesterification of Vegetable Oils: A Review. Proc. 2012 Mech. Eng. Conf. Sustain. Res. Innov. 4, 59–68.

Kumari, P., Reddy, C.R.K., Jha, B., 2011. Comparative evaluation and selection of a method for lipid and fatty acid extraction from macroalgae. Anal. Biochem. 415, 134–144.

Lam, M.K., Lee, K.T., Mohamed, A.R., 2010. Homogeneous, heterogeneous and enzymatic catalysis for transesterification of high free fatty acid oil (waste cooking oil) to biodiesel: A review. Biotechnol. Adv.

Maceiras, R., Rodrí guez, M., Cancela, A., Urréjola, S., Sánchez, A., 2011. Macroalgae: Raw material for biodiesel production. Appl. Energy 88, 3318–3323

Moosavi, R., Ramanathan, S., Lee, Y.Y., Siew Ling, K.C., Afkhami, A., Archunan, G., Padmanabhan, P., Gulyás, B., Kakran, M., Selvan, S.T., 2015. Synthesis of antibacterial and magnetic nanocomposites by decorating graphene oxide surface with metal nanoparticles. RSC Adv. 5, 76442–76450.

Ngamcharussrivichai, C., Totarat, P., Bunyakiat, K., 2008. Ca and Zn mixed oxide as a heterogeneous base catalyst for transesterification of palm kernel oil. Appl. Catal. A Gen. 341, 77–85.

Noiroj, K., Intarapong, P., Luengnaruemitchai, A., Jai-In, S., 2009. A comparative study of KOH/Al2O3 and KOH/NaY catalysts for biodiesel production via transesterification from palm oil. Renew. Energy 34, 1145–1150.

Ojha, M.L., Chadha, N.K., Saini, V.P., Damroy, S., Gupta, C.P., Savant, P.B., 2014. Effect of ethanolic extract of pedalium murex on growth and haemato-immunological parameters of Labeo rohita. Proc. Natl. Acad. Sci. India Sect. B - Biol. Sci. 84, 997–1003.

Patel, D.K., Laloo, D., Kumar, R., Hemalatha, S., 2011. Pedalium murex Linn.: An overview of its phytopharmacological aspects. Asian Pac. J. Trop. Med. 4, 748–755.

Rajkumari, J., Maria, Magdalane C., Siddhardha, B., Madhavan, J., Ramalingam, G., Al-Dhabi, N.A., Arasu, M.V., Ghilan, A.K.M., Duraipandiayan, V., 2019. Kaviyarasu K. Synthesis of titanium oxide nanoparticles using Aloe barbadensis mill andevaluation of its antibiofilm potential against Pseudomonas aeruginosa PAO1. J. Photochem. Photobiol., B. https://doi.org/10.1016/j.jphotobiol.2019.111667.

Reyero, I., Arzamendi, G., Gandía, L.M., 2014. Heterogenization of the biodiesel synthesis catalysis: CaO and novel calcium compounds as transesterification catalysts. Chem. Eng. Res. Des. 92, 1519–1530.

Ruparelia, J.P., Chatterjee, A.K., Duttagupta, S.P., Mukherji, S., 2008. Strain specificity in antimicrobial activity of silver and copper nanoparticles. Acta Biomater. 4, 707–716.

S.Hawash, G.El Diwani, E.A.K., 2011. Optimization of Biodiesel Production from Jatropha Oil By Heterogeneous Base Catalysed Transesterification. Int. J. Eng. Sci. Technol. 3, 5242–5251.

Satyarthi, J.K., 2011. Catalytic Conversion of Vegetable Oils To Biofuels Over Transition Metal Catalysts.

Shao, W., Liu, X., Min, H., Dong, G., Feng, Q., Zuo, S., 2015. Preparation, characterization, and antibacterial activity of silver nanoparticle-decorated graphene oxide nanocomposite. ACS Appl. Mater. Interfaces 7, 6966–6973.

SHARMA, P.R.S., n.d. In vivo and in vitro biochemical investigation of primary metaboli from pedalium murex. Int. J. Res. Rev. Pharm. Appl. Sci. 2, 550–555.

Sharma, V., Thakur, M., Dixit, V.K., 2012. A comparative study of ethanolic extracts of Pedalium murex Linn. fruits and sildenafil citrate on sexual behaviors and serum testosterone level in male rats during and after treatment. J. Ethnopharmacol. 143, 201–206.

Shrivastava, S., Bera, T., Roy, A., Singh, G., Ramachandrarao, P., Dash, D., 2010. Characterization of enhanced antibacterial effects of novel silver nanoparticles. Nanotechnology 18, 1–9.

Sivaprakash, G., Mohanrasu, K., Ananthi, V., Jothibasu, M., Nguyen, D.D., Ravindran, B., Chang, S.W., Nguyen-Tri, P., Tran, N.H., Sudhakar, M., Gurunathan, K., Arokiyaraj, S., Arun, A., 2019. Biodiesel production from Ulva linza, Ulva tubulosa, Ulva fasciata, Ulva rigida, Ulva reticulate by using Mn2ZnO4 heterogenous nanocatalysts. Fuel 255, 115744.

Tang, J., Chen, Q., Xu, L., Zhang, S., Feng, L., Cheng, L., Xu, H., Liu, Z., Peng, R., 2013. Graphene oxide-silver nanocomposite as a highly effective antibacterial agent with species-specific mechanisms. ACS Appl. Mater. Interfaces 5, 3867–3874.

Umdu, E.S., Tuncer, M., Seker, E., 2009. Transesterification of Nannochloropsis oculata microalga's lipid to biodiesel on Al2O3 supported CaO and MgO catalysts. Bioresour. Technol. 100, 2828–2831.

Valsalam, S., Agastian, P., Arasu, M.V., Al-Dhabi, N.A., Ghilan, A.K.M., Kaviyarasu, K., Ravindran, B., Chang, S.W., Arokiyaraj, S., 2019a. Rapid biosynthesis and characterization of silver nanoparticles from the leaf extract of Tropaeolum majus L. and its enhanced in-vitro antibacterial, antifungal, antioxidant and anticancer properties. J. Photochem. Photobiol., B 191, 65–74.

Valsalam S, Agastian P, Esmail. GA., Ghilan AKM, Al-Dhabi NA, Arasu MV. Biosynthesis of silver and gold nanoparticles using Musa acuminata colla flower and its pharmaceutical activity against bacteria and anticancer efficacy. Journal of Photochemistry & Photobiology, B: Biology: 2019b. doi.org/10.1016/j.jphotobiol.2019.111670.

Vijayan, S.R., Santhiyagu, P., Singamuthu, M., Kumari Ahila, N., Jayaraman, R., Ethiraj, K., 2014. Synthesis and characterization of silver and gold nanoparticles using aqueous extract of seaweed, turbinaria conoides, and their antimicrofouling activity. Sci. World J. 2014.

Wu, H., Zhang, Junhua, Wei, Q., Zheng, J., Zhang, Jianan, 2012. Transesterification of soybean oil to biodiesel using zeolite supported CaO as strong base catalysts. Fuel Process, Technol.

Yoldas, B.E., 1975. Alumina gels that form porous transparent Al2O3. J. Mater. Sci. 10, 1856–1860.

Zabeti, M., Daud, W.M.A.W., Aroua, M.K., 2009. Optimization of the activity of CaO/Al2O3 catalyst for biodiesel production using response surface methodology. Appl. Catal. A Gen. 366, 154–159.

Zabeti, M., Daud, W.M.A.W., Aroua, M.K., 2010. Biodiesel production using alumina-supported calcium oxide: An optimization study. Fuel Process. Technol. 91, 243–248.